ACS OMEGA

Open Access

http://pubs.acs.org/journal/acsodf

Article

Theoretical Study of Ground-State Barium−Rare Gas Van der Waals Complexes: Combining Rule Modeling and Ab Initio Calculations

Samah Saidi,* Mohamed Bejaoui,* and Hamid Berriche*

Cite This: *ACS Omega* 2024, 9, 32407−32417

Read Online

ACCESS | Metrics & More | Article Recommendations | Supporting Information

ABSTRACT: The present study aims to generate the potential energy curves (PECs) and spectroscopic constants for barium alkaline earth (AE) atoms interacting with rare gas (RG) atoms (He, Ne, Ar, Kr, and Xe). The study focuses on investigating the van der Waals bonds that characterize the interactions between alkaline-earth metals and RG atoms, with a specific emphasis on employing the Tang and Toennies (TT) potential model, known to accurately describe such interactions. The TT potential model was employed in conjunction with combining rules to calculate its parameters, which include dispersion coefficients C_{2n} and Born−Mayer constants A and b. Additionally, we have conducted high-level ab initio calculations at the CCSD(T) level for all Ba−RG ground states. Obtained PECs from both methods have been used to evaluate the spectroscopic properties D_e, R_e, ω_e, B_e, and $\omega_e\chi_e$. Our findings reveal that the derived spectroscopic constants from the TT model exhibit good agreement with the results obtained from CCSD(T) calculations and with other available theoretical studies. Furthermore, to gain insights into the relative differences among AE−RG species, we calculated the κ parameter for AE−RG and AE^+−RG (AE = Sr, Ca, Mg, Ba; RG = He−Xe) complexes. It is found that except for the case of Ba−RG and Ba^+−RG, the κ values within the same series, AE−RG and AE^+−RG, are remarkably close to each other.

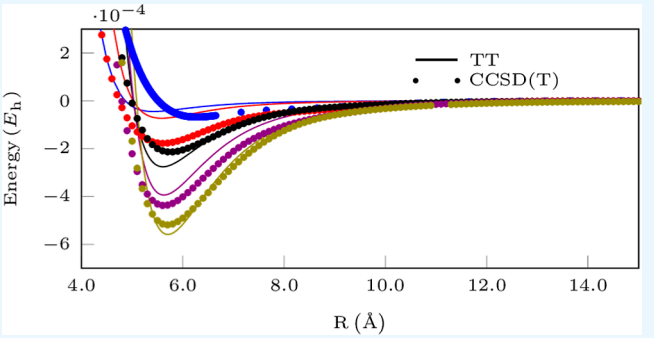

1. INTRODUCTION

Recently, barium alkaline earth (AE) metals interacting with rare gas (RG) atoms have attracted the interest of an important number of researchers. This is due to its significant potential for both fundamental research and practical applications. One notable application is related to a crucial role played by matrix isolation spectroscopy (MIS) in detecting single barium (Ba) atoms in solid xenon (Xe) for the nEXO project.[1] This technique enables the unique identification of individual barium atoms in a solid xenon matrix, which is essential for the nEXO project's goal of searching for neutrinoless double beta ($0\nu\beta\beta$) decay with a high sensitivity.[1,2] This significant application of MIS has sparked interest in exploring the behavior of atomic barium within inert gas matrices. Recently, a study utilizing two-dimensional excitation−emission (2D-EE) spectroscopy and absorption spectroscopy has been conducted to characterize the luminescence of atomic barium isolated in krypton (Kr), argon (Ar), and xenon (Xe) RG solids.[3−5] This research has offered detailed insights into the distinct sites occupied by atomic barium in these RG hosts. Furthermore, investigation of barium in He-nanodroplets,[6,7] in solid and liquid helium,[8] and isolated on large RG clusters[9,10] has provided insights into excited P states forming bubbles in liquid helium or size exclusion effects, compelling surface attachment on argon clusters.

In previous studies, a series of experiments have been conducted to investigate atomic collision processes involving barium and RG atoms. Measurements of pressure-broadening effects on the barium atom have been reported in a series of papers.[11−13] Breckenridge and Merrow[14] and Visticot et al.[15] have conducted a spin-changing collision involving the barium atom. Excitation transfer among low-lying excited states of the Ba atom induced by collisions with RG atoms has been explored by Ehrlacher and Huennekens,[16] Vadla et al.,[17] and Brust and Gallagher.[18] Namiotka et al.[19] conducted experiments to measure the diffusion of ground-state and lowest ^3D_j metastable-state barium atoms in a buffer gas. Smedley et al.[20] have investigated the collisional deactivation of barium by noble gases employing the wavelength-resolved fluorescence techniques.

Knowledge of reliable interatomic potential energy curves (PECs) for Ba−RG diatomic systems is crucial for understanding the results of the various mentioned experiments, especially the calculations for the appropriate collisional cross sections. Czuchaj et al.[21] conducted pioneering investigations

Received: November 2, 2023
Revised: April 1, 2024
Accepted: April 25, 2024
Published: July 22, 2024

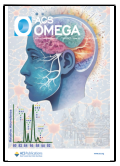

into these complexes, utilizing the pseudopotential approach to integrate the two-electron Ba and eight (valence)-electron RG descriptions. More recently, computations for Ba−Ar,[22] Ba−Xe,[23] and Ba−Kr[24] have followed a similar theoretical approach with two electrons, revealing a significant deviation for the ground state of Ba−Xe. Davis and McCaffrey[5] and Buchachenko and Viehland[25] have employed the CCSD(T) method to calculate interaction potentials of Ba with Ar, Kr, and Xe and Ba, Ba^+, and Ba^{2+} interacting with RG atoms from He to Xe, respectively. Recently, Xian et al.[26] have used the CCSD(T) theory with spin−orbit coupling (SOC) to study the spectroscopic properties of the ground state of the diatomic Ba−RG (RG = Kr, Xe, Rn).

Despite significant progress in modern computer techniques, ab initio calculations on weakly bound van der Waals systems continue to challenge computational chemists. Therefore, developing models to address these weak interactions continues to offer an interesting alternative. The Tang and Toennies (TT) model potential[27] is widely used to handle van der Waals diatomic systems. It has been employed effectively to interpret the interactions among all 21 possible combinations of homogeneous and heterogeneous pairs of RG atoms[28] and group 2 (Mg_2, Ca_2, Sr_2, and Ba_2) pairs.[29−32] Furthermore, by employing this model and well-established sets of combining rules, the parameters C_6, C_8, C_{10}, A, and b for mixed pairs X−RG (X = Hg, Zn Sr, Ca, Mg; RG = He−Xe)[30,31,33−35] were determined from the parameters of homonuclear dimers X_2 and RG_2.

Given the success of the TT model potential in previous studies, where it was effectively applied in generating homonuclear dimers of rare gas (RG_2)[27,36−39] and barium Ba_2,[32] as well as its effectiveness with a specific set of combining rules for generating interactions involving heterogeneous X−RG pairs,[30,31,33−35] we hypothesize that this model, along with the same set of combining rules, can accurately describe the van der Waals interactions within the Ba−RG complexes (RG = He−Xe). In the current work, the TT potential model[27] will be employed in conjunction with combining rules to calculate its parameters, including dispersion coefficients and Born−Mayer constants. Additionally, as most of the ab initio results used for comparison are relatively old, alongside the used TT model, we have conducted high-level ab initio calculations at the (CCSD(T)) level of theory for all Ba−RG ground states, employing extensive basis sets.

This manuscript is structured as follows: Section 2 delves into the TT model and the combining-rules approach, which are employed to generate short- and long-range parameters (A, b, C_6, C_8, and C_{10}) for Ba−RG complexes. The results are presented and discussed in Section 3, where we conduct a comparative analysis of the spectroscopic constants D_e, R_e, ω_e, B_e, and $\omega_e\chi_e$ with previous existing studies and the present ab initio calculations. Section 4 is dedicated to the exploration of κ parameters for AE−RG and AE^+−RG (AE = Sr, Ca, Mg, Ba; RG = He−Xe) complexes.

2. METHOD

2.1. Model Potential. Tang and Toennies model potential (TT), originally proposed in 1984 by Tang and Toennies,[27] is widely regarded as the most suitable model for describing van der Waals interactions of the X−RG type, where X represents AE and RG represents noble gas. This study focuses on examining Ba−RG (barium−rare gas) interactions. It represents an extension of the initial study proposed by one of these authors[40] in 1973. In the earlier model, the Born−Mayer repulsive potential[41] $[A\exp(-bR)]$ with parameters derived from self-consistent field calculations is added to the first three terms of the asymptotically $(R \to \infty)$ correct ab initio dispersion.

$$V(R) = V_{SCF}(R) - \sum_{n=3}^{n_{max}} \frac{C_{2n}}{R^{2n}} \tag{1}$$

Despite its straightforward nature, this model proves to be highly effective in accurately describing the experimental potentials for RG dimers. To account for the impact of charge overlap on the dispersion interaction within the attractive component, Tang and Toennies introduced the $f_{2n}(bR)$ damping function into the long-range dispersion terms.[27] Consequently, eq 1 is modified as follows

$$V(R) = A\, e^{(-bR)} - \sum_{n=3}^{n_{max}} f_{2n}(bR)\frac{C_{2n}}{R^{2n}} \tag{2}$$

where R is the internuclear distance, A and b are the parameters governing the Born−Mayer repulsive potential,[41] and C_{2n} are the dispersion coefficients. The function $f_{2n}(bR)$, as described in eq 3, serves as the radial-dependent damping function for individual dispersion coefficients C_{2n}.

$$f_{2n}(bR) = 1 - e^{(-bR)} \sum_{k=0}^{2n} \frac{(bR)^k}{k!} \tag{3}$$

It is worth noting that the coefficient b is the same as the short-range parameter in the Born−Mayer repulsion. This similarity arises from the fact that both the repulsion and dispersion damping functions stem from the overlap of wave functions.

The subsequent section is devoted to presenting the combining rules approach, which will be employed to determine the potential for mixed systems ij based on the known parameters of the homonuclear systems ii and jj. These parameters will be utilized within the Tang and Toennies model to accurately predict the potential for heteronuclear combinations of barium−rare gas dimers.

2.2. Combining Rules. *2.2.1. Combining Rules for A and b.* In the context of determining the short-range Born−Mayer repulsive coefficients A and b for a mixed system ij, there exist several rules[42−45] that facilitate their calculation based on the parameters of two known systems ii and jj. In the present study, the i and j indices stand for the parameters of AE and RG homonuclear dimers. Among these rules, the four equations (eqs 30−33 in ref 45) tested by Böhm−Ahlrichs[45] are commonly used. It is important to note that despite variations in the results obtained from each equation, all of them have proven to be valuable. As combining rules rely on empirical reasoning, the method's reliability is ultimately assessed by its ability to accurately predict potential interactions between pairs of atoms.

In this study, we have adopted a specific set of combining rules, detailed below, which are related to eq 31 in ref 45. We anticipate that these rules are the most suitable for all AE−RG interactions. Our choice is substantiated by the work conducted by Yang and co-workers[30] and Yin and co-workers,[31] as well as our previous research.[34] This approach has demonstrated great success when applied to interactions involving magnesium, calcium, and strontium with RG atoms.[30,31,34]

https://doi.org/10.1021/acsomega.3c08696
ACS Omega 2024, 9, 32407−32417

Table 1. Potential Parameters of Ba−RG Derived from Combining Rules[a]

system	C_6	C_8	C_{10}	A	b
Ba−Ar	371.650081	30,554.2512	2,844,308.72	280.839492	1.30070469
Ba−He	48.0676549	3572.93879	319,663.418	66.5025112	1.38659845
Ba−Kr	550.781072	46,696.3446	4,377,717.63	296.200878	1.26475191
Ba−Ne	93.6513311	7106.58825	650,104.266	145.007931	1.37732076
Ba−Xe	876.222568	76,948.8778	6,970,832.43	316.732884	1.21940532

[a]All values are in au.

Table 2. Theoretical Parameters of Ba−RG Used in the Present Work[a]

system	α_1	α_2	α_3	C_6	C_8	C_{10}	A	b
He−He	1.383	2.443	10.603	1.461	14.11	183.6	41.96	2.523
Ne−Ne	2.66	6.42	30.4	6.383	90.34	1536	199.5	2.458
Ar−Ar	11.1	52.4	490	64.30	1623	49,060	748.3	2.031
Kr−Kr	16.7	92.7	793	129.6	4187	155,500	832.4	1.865
Xe−Xe	27.3	170	2016	285.9	12,810	619,800	951.8	1.681
Ba−Ba	272.1	8900	206,000	5160	772,000	101,400,000	105.4	0.9567

[a]All values are in au.

$$A_{ij} = [A_i A_j]^{1/2}, \qquad b_{ij} = 2\frac{b_i b_j}{b_i + b_j} \tag{4}$$

Table 1 presents the values of parameters A and b for the barium−rare gas complexes, which were obtained using data from barium[32] and RG[28] dimers provided in Table 2, employing the combining rules approach.

2.2.2. Combining Rules for C_6, C_8, and C_{10}. For C_6, C_8, and C_{10}, the combining rules rely on the principles of the Casimir−Polder theory for dispersion coefficients. This theory involves deriving dispersion coefficients from the various terms arising in the multipole expansion of the perturbation operator, as outlined in the Casimir−Polder theory of dispersion coefficients.[46,47]

$$C_6 = C^{ij}(1, 1) \tag{5}$$

$$C_8 = C^{ij}(1, 2) + C^{ij}(2, 1) \tag{6}$$

$$C_{10} = C^{ij}(1, 3) + C^{ij}(2, 2) + C^{ij}(3, 1) \tag{7}$$

where $C^{ij}(1, 2)$, $C^{ij}(2, 2)$, and $C^{ij}(1, 3)$ represent, respectively, the dipole−dipole, the dipole−quadrupole, the quadrupole−quadrupole, and the dipole−octupole interaction. Each of these terms $C^{ij}(l_1, l_2)$ is precisely defined by the following exact formula[46−48]

$$C^{ij}(l_1, l_2) = \frac{(2l_1 + 2l_2)!}{4(2l_1)!(2l_2)!}\left(\frac{2}{\pi}\right)\int_0^\infty \alpha_{l_1}^i(\mathrm{i}\omega)\alpha_{l_2}^j(\mathrm{i}\omega)\mathrm{d}\omega \tag{8}$$

where $\alpha_{l_1}^i(\mathrm{i}\omega)$ and $\alpha_{l_2}^j(\mathrm{i}\omega)$ are the dynamic multipole polarizabilities of atoms i and j at the frequency ω, respectively. It should be noted that this expression involves an integral across imaginary frequencies, representing the product of the dynamic polarizabilities of the interacting atoms. This formulation simplifies the initial two-centered problem into a one-centered problem, which entails evaluating the frequency-dependent polarizabilities. To approximate the dynamic dipole polarizability $\alpha_l(\mathrm{i}\omega)$, a one-term approximant proposed by Tang $[\alpha_l(\mathrm{i}\omega)]$ should be introduced[49]

$$[\alpha_l(\mathrm{i}\omega)] = \frac{\alpha_l}{1 + (\omega/\Omega_l)^2}, \qquad l = 1, 2, 3 \tag{9}$$

We note that α_l is the static polarizability $\alpha_l(0)$ and Ω_l is the effective energy. Using this approximation and the well-known mathematical identity[50]

$$\frac{2}{\pi}\int_0^\infty \frac{ab}{(a^2 + \omega^2)(b^2 + \omega^2)}\mathrm{d}\omega = \frac{1}{a^2 + b^2} \tag{10}$$

it can be shown that

$$C^{ij}(1, 1) = \frac{3}{\Pi}\int_0^\infty [\alpha_1^i(\mathrm{i}\omega)][\alpha_1^j(\mathrm{i}\omega)] = \frac{3}{2}\left[\frac{\alpha_1^i\alpha_1^j\Omega_1^i\Omega_1^j}{\Omega_1^i + \Omega_1^j}\right] \tag{11}$$

Similarly

$$C^{ij}(1, 2) = \frac{15}{4}\left[\frac{\alpha_1^i\alpha_2^j\Omega_1^i\Omega_2^j}{\Omega_1^i + \Omega_2^j}\right] \tag{12}$$

$$C^{ij}(1, 3) = 7\left[\frac{\alpha_1^i\alpha_3^j\Omega_1^i\Omega_3^j}{\Omega_1^i + \Omega_3^j}\right] \tag{13}$$

$$C^{ij}(2, 2) = \frac{35}{2}\left[\frac{\alpha_2^i\alpha_2^j\Omega_2^i\Omega_2^j}{\Omega_2^i + \Omega_2^j}\right] \tag{14}$$

For many systems, the static polarizability $\alpha_l(0)$ is available. To compute the required effective energy value Ω_l, we employ the formula for the homonuclear dipole−dipole interaction. Consequently, eq 11 simplifies to eq 15

$$C_6^i = C^{ii}(1, 1) = \frac{3}{4}(\alpha_1^i)^2\Omega_1^i \tag{15}$$

where the single index i represents the homonuclear dimer. This results in the following expression

$$\Omega_1^i = \frac{4}{3(\alpha_1^i)^2}C_6^i \tag{16}$$

According to Tang's theorem,[49] the approximant $[\alpha_1^i(\mathrm{i}\omega)]$ with this Ω_1^i must intersect $\alpha_1^i(\mathrm{i}\omega)$ once and only once beside $\omega = 0$. Therefore, the combining rule obtained by substituting eq 16 into 11 yields very precise coefficients

https://doi.org/10.1021/acsomega.3c08696
ACS Omega 2024, 9, 32407−32417

$$C_6^{ij} = C^{ij}(1, 1) = \frac{2\alpha_1^i\alpha_1^j C_6^i C_6^j}{(\alpha_1^i)^2 C_6^j + (\alpha_1^j)^2 C_6^i} \tag{17}$$

Tang demonstrated the validity of this approach using a select set of representative interactions.[49] Applying the same underlying principle, precise combining rules for C_8 and C_{10} can be derived.[51] In homonuclear interactions, $C^i(l_1, l_2) = C^i(l_2, l_1)$. With $C_8^i = 2C^{ii}(1, 2)$, the effective energy Ω_2^i can be computed using eq 12

$$\Omega_2^i = \frac{2C_8^i\Omega_1^i}{15\alpha_1^i\alpha_2^i\Omega_1^i - 2C_8^i} \tag{18}$$

Solving for Ω_3^i from eq 13, we get

$$\Omega_3^i = \frac{C^i(1, 3)\Omega_1^i}{7\alpha_1^i\alpha_3^i\Omega_1^i - C^i(1, 3)} \tag{19}$$

where $C^i(1, 3)$ can be expressed as

$$C^i(1, 3) = \frac{1}{2}[C_{10}^i - C^i(2, 2)] = \frac{1}{2}\left[C_{10}^i - \frac{35}{4}(\alpha_2^i)^2\Omega_2^i\right] \tag{20}$$

Utilizing the homonuclear dispersion coefficient C_6^i, C_8^i, C_{10}^i and the polarizabilities α_1^i, α_2^i, α_3^i allows us to determine the three effective energies Ω_1^i, Ω_2^i, Ω_3^i. Subsequently, we can calculate the heteronuclear coefficients C_6^{ij}, C_8^{ij} and C_{10}^{ij} using eqs 5−7.

In this study, we apply the aforementioned expressions to compute the dispersion coefficients for the heteronuclear Ba−RG systems. For homonuclear RG pairs, we obtain the necessary values of C_6^i, C_8^i, C_{10}^i from ref 28 and the polarizabilities α_1^i, α_2^i, α_3^i from ref 51. Meanwhile, for the barium pairs, we take the polarizabilities and dispersion coefficients from ref 52. All the essential coefficients are provided in Table 2. The resulting dispersion coefficients C_6, C_8, and C_{10} for Ba−RG, obtained through the combining rules approach, are summarized in Table 1.

2.3. Reduced Potential and Spectroscopic Constants.

Five parameters, A, b, C_6, C_8, and C_{10}, are good enough to describe the potential energy of Ba−RG employing the TT model provided by eq 2. Once the PECs of the Ba−RG systems are derived, their equilibrium distances and well depths are easily extracted.

For diatomic molecules, the energy of vibrotational levels is expressed by the following equation

$$E(v, J) = \sum_{i,j} Y_{ij}\left(v + \frac{1}{2}\right)^i\left(J\left(\left(J + \frac{1}{2}\right)^j\right)\right) \tag{21}$$

The Y_{ij} coefficients are the widely recognized Dunham coefficients,[53] and the ω_e, B_e, and $\omega_e\chi_e$ spectroscopic constants are linked to these coefficients by the following relationships

$$Y_{10} \approx \omega_e \tag{22}$$

$$Y_{20} \approx \omega_e\chi_e \tag{23}$$

$$Y_{01} \approx B_e \tag{24}$$

where ω_e is the classical frequency, $\omega_e\chi_e$ is the anharmonicity, and B_e is the vibrotational coupling constant. The precise expressions for Y_{10}, Y_{20}, and Y_{11} are provided by Dunham.[54]

To calculate the unknown spectroscopic constants and explore the shape of the potentials, it is suitable to represent the interaction potential $V(R)$ in a reduced form.

If

$$x = \frac{R}{R_e} \text{ and } U(x) = V(R_e x)/D_e \tag{25}$$

therefore

$$V(R) = A^* e^{-b^* x} - \sum_{n=3}^{n_{max}} f_{2n}^*(x)\frac{C_{2n}^*}{x^{2n}} \tag{26}$$

where

$$f_{2n}^*(x) = 1 - e^{-b^* x} - \sum_{k=0}^{2n}\frac{(b^* x)^k}{k!} \tag{27}$$

$$C_{2n}^* = \frac{C_{2n}}{D_e R_e^{2n}} \tag{28}$$

$$b^* = bR_e, \qquad A^* = \frac{A}{D_e} \tag{29}$$

Expanding the $U(x)$ function around R_e, the equilibrium distance, in a power series relative to x (where $x = R/R_e$), allows us to express the spectroscopic parameters in terms of the following coefficients

$$U(x) = -1 + a_0(x - 1)^2 + (1 + a_1(x - 1) + a_2(x - 1)^2 ...) \tag{30}$$

The coefficients a_n of the power series expansion are determined as follows

$$a_0 = \frac{1}{2}U^{(2)}(1), \qquad a_1 = \frac{1}{3}\frac{U^{(3)}(1)}{U^{(2)}(1)}, \qquad a_2 = \frac{1}{12}\frac{U^{(4)}(1)}{U^{(2)}(1)}, \ ... \tag{31}$$

Hence, we can express the following three dimensionless quantities in terms of the expansion coefficients a_n[54,55]

$$\frac{B_e D_e}{\omega_e^2} = \frac{1}{4a_0} \tag{32}$$

$$\frac{\alpha_e\omega_e}{B_e^2} = -6(1 + a_1) \tag{33}$$

$$\frac{\omega_e\chi_e}{B_e} = -\frac{3}{2}\left(a_2 - \frac{5}{2}a_1^2\right) \tag{34}$$

with

$$B_e = \frac{h}{8\pi^2\mu c R_e^2} \tag{35}$$

become in terms of atomic units

$$B_e = \frac{1}{2\mu R_e^2} \tag{36}$$

The reduced mass μ and the equilibrium distance R_e are expressed in atomic units; 1 amu = $1822.8m_e$, where m_e is the mass of the electron which is equal to one in atomic units.

To evaluate $U^{(2)}(1)$, $U^{(3)}(1)$, and $U^{(4)}(1)$, we should define

$$U^n(x) = \frac{d^n U(x)}{dx^n} \tag{37}$$

https://doi.org/10.1021/acsomega.3c08696
ACS Omega 2024, 9, 32407−32417

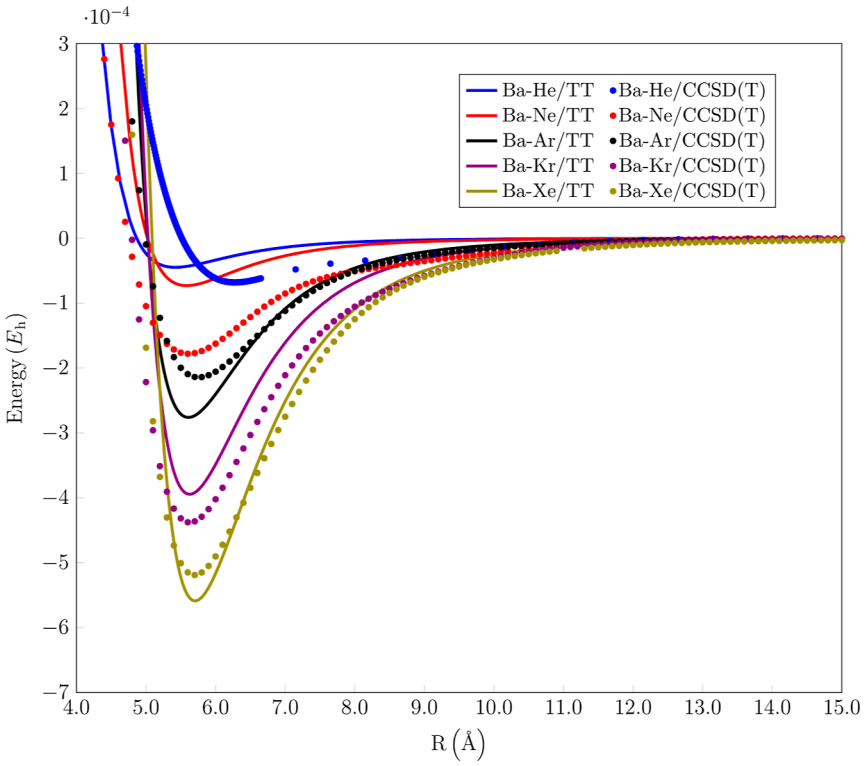

Figure 1. Van der Waals potentials for Ba−RG (RG = He, Ne, Ar, Kr, Xe) ground states obtained by using CCSD(T) and the TT potential model.

At the equilibrium distance $x = 1$, the reduced potential provides us with two conditions

$$U(1) = -1 \tag{38}$$

$$U^{(1)}(1) = 0 \tag{39}$$

so

$$U^{(2)}(1) = b^{*2}A^* \, e^{-b^*} + \sum_{n=3}^{n_{max}} e^{-b^*}(b^{*2} + 2nb^*)\frac{(b^*)^{2n}}{(2n)!}C_{2n}^* - \sum_{n=3}^{n_{max}}\left[1 - e^{-b^*}\sum_{k=0}^{2n}\frac{(b^*)k}{k!}\right]2n(2n+1)C_{2n}^* \tag{40}$$

$$U^{(3)}(1) = -b^{*3}A^* \, e^{-b^*} - \sum_{n=3}^{n_{max}} e^{-b^*}(b^{*3} + 2nb^{*2} + 4n(n+1)b^*)\frac{(b^*)^{2n}}{(2n)!}C_{2n}^* + \sum_{n=3}^{n_{max}}\left[1 - e^{-b^*}\sum_{k=0}^{2n}\frac{(b^*)^k}{k!}\right]2n(2n+1)(2n+2)C_{2n}^* \tag{41}$$

$$U^{(4)}(1) = -b^{*4}A^* \, e^{-b^*} + \sum_{n=3}^{n_{max}} e^{-b^*}[(b^{*4} + 2nb^{*3} + 2n(2n+3)b^{*2} + 4n(n+1)(2n+3)b^*)]\frac{(b^*)^{2n}}{(2n)!}C_{2n}^* - \sum_{n=3}^{n_{max}}\left[1 - e^{-b^*}\sum_{k=0}^{2n}\frac{(b^*)^k}{k!}\right]2n(2n+1)(2n+2)(2n+3)C_{2n}^* \tag{42}$$

Using these derivatives, we can determine the a_n. Therefore, from eqs 31 to 34, the spectroscopic constants (ω_e, $\omega_e\chi_e$, and B_e) can be easily derived using D_e, R_e, a_0, a_1, and a_2.

2.4. Ab Initio Calculation. In addition to the used TT model potential, we conducted ab initio calculations for all Ba−RG pairs using the coupled cluster method with double and triple excitations (CCSD(T)), along with appropriate basis sets. For the atoms He, Ne, Ar, and Kr, we employed the standard aug-cc-pV5Z[56−60] and aug-cc-pV6Z basis sets.[56−58,61,62] For the Xe atom, the basis set employed was the standard ECP + valence,[63,64] ECP28MDF-aV5Z. In the case of the barium (Ba) atom, the dhf-TZVPP pseudo potential[65−68] along with its corresponding basis set was used in the calculations for Ba−He, Ba−Ne, and Ba−Kr. For Ba−Ar and Ba−Xe, an ECP46MDF pseudopotential basis set[63,68] was utilized.

All calculations were conducted using the MOLPRO 2010 quantum chemistry package.[69] These calculations were performed with rigorous convergence criteria involving large basis sets and pseudopotentials, which ensured a high degree of accuracy in determining the electronic structure and properties of these diatomic molecules. To achieve a higher level of accuracy, strict convergence criteria were applied, including a

https://doi.org/10.1021/acsomega.3c08696
ACS Omega 2024, 9, 32407−32417

Table 3. Comparison of the Spectroscopic Constant of the Van der Waals Ground-State Potentials of the Barium−Rare Gas Complexes with Other Available Results

	R_e (Å)	D_e (cm^{-1})	ω_e (cm^{-1})	$\omega_e\chi_e$ (cm^{-1})	B_e (cm^{-1})	ref
Ba−He	5.45	10	21.08	11.10	0.150059	TT
	6.27	14.96	17.66	5.21	0.110114	CCSD(T)
	6.651	2.6	1.10		0.077	ECP/CBS/(CCSD(T))[25]
	5.70	8.74				surface integral[70]
	6.40	5				pseudopotential[71]
	5.80	3.5				pseudopotential[72]
Ba−Ne	5.58	16	7.99	8.50	0.030093	TT
	5.61	39.07	10.53	0.71	0.030444	CCSD(T)
	5.815	12.0	6.8	0.99	0.0267	ECP/CBS/(CCSD(T))[25]
	5.34	64	22			CI/pseudopotential[21]
Ba−Ar	5.61	60	13.75	1.15	0.017309	TT
	5.75	47.03	9.26	0.46	0.016448	CCSD(T)
	5.482	62.9	11.3	0.51	0.0178	ECP/CBS/(CCSD(T))
	5.62	54.2				ECP CCSD(T)[73]
	5.56	73	16			CI/pseudopotential[21]
	5.36	72.7	11.1			pseudopotential[22]
Ba−Kr	5.63	87	11.97	0.88	0.010220	TT
	5.62	96.10	9.87	0.25	0.010223	CCSD(T)
	5.387	101.4	10.6	0.27	0.0110	ECP/CBS/(CCSD(T))[25]
	5.57	84.0				ECP CCSD(T)[73]
	5.72	80	13			CI/pseudopotential[21]
Ba−Xe	5.70	123	12.17	0.66	0.007711	TT
	5.69	113.88	9.40	0.19	0.007741	CCSD(T)
	5.450	147.9	11.0	0.19	0.0084	ECP/CBS/(CCSD(T))[25]
	5.55	131.1				ECP CCSD(T)[73]
	5.93	101	11			CI/pseudopotential[21]
	5.11	427	17	0.546	0.00950	pseudopotential[23]

10^{-14} E_h threshold for energy convergence, a threshold of 10^{-8} for orbital convergence, and a threshold of 10^{-7} for CI vector convergence. The resulting PECs are presented in Figure 1. To facilitate a relative comparison of the well depth and equilibrium distance, these curves were adjusted so that their final point was set to zero E_h. Table 3 summarizes the spectroscopic constants.

3. RESULTS AND DISCUSSION

3.1. PECs and Spectroscopic Parameters. Figure 1 illustrates the PECs for Ba−RG (RG = He−Xe) resulting from both the ab initio CCSD(T) calculation (the detailed potential energy data are provided in the Supporting Information) and the TT model potential, considering dispersion series up to $n_{max} = 5$ and employing parameters from Table 1. It is noted that both results display a similar trend in the potential well depth (D_e), which consistently increases as the size of the rare gas atoms increases from He to Xe. Additionally, a comparison of the displayed TT PECs of Ba−RG with those of Ca−RG, Sr−RG, and Mg−RG, generated with the same method and displayed in Figure 3 of ref 30, Figure 3a of ref 31, and Figure 1 of ref 34, respectively, reveals similar behavior in the potential well depth. The associated equilibrium position (R_e(Å) = 5.45, 5.58, 5.61, 5.63, 5.70) increases very little from one system to another.

On the other hand, it can be seen from Figure 1 that the TT model potentials effectively describe the long-range portion of the ab initio CCSD(T)PECs. However, their performance weakens considerably on the repulsive inner wall. This behavior can be attributed to the TT formalism itself. The long-range portion is very reliable because the dispersion coefficients are computed by using the well-established combining rules. In contrast, the repulsive part relies on a simple Born−Mayer potential [$A \exp(-bR)$] added to the attractive potential. Tang et al.[31] recognize that the combining rules of eq 4 for the Born−Mayer parameters are not as precise, a fact starkly evident on comparison with the high-level CCSD(T) results. Regarding the potential well region, better agreement is observed between the TT and the present CCSD(T) curves for Ba−Ar, Ba−Kr, and Ba−Xe, while noticeable differences are observed for Ba−He and modest agreement is observed for Ba−Ne. This discrepancy can be attributed to the weak binding of Ba−Ne and, especially, Ba−He, which poses a challenge for both TT and CCSD(T).

A comparison of the derived spectroscopic constants D_e, R_e, ω_e, B_e, and $\omega_e\chi_e$ from TT potential, with both present ab initio CCSD(T) and previous theoretical determinations, is provided in Table 3. Inspection of these results reveals that the interactions within the Ba−RG complexes (RG = He−Xe) are characterized by very weak binding. This observation aligns with the well-established understanding of the ground state's weakly bound nature in atom−rare gas pairs.[73] Furthermore, the depth of the potentials increases as the RG atomic mass rises, a consequence of the growing polarizability of noble gas atoms from He to Xe. The Ne/He, Ar/Ne, Kr/Ar, and Xe/Kr polarizability ratios are, 1.93, 4.15, 1.53, and 1.61, respectively; the corresponding ratios of the $D_eR_e^4$ values are 1.77, 3.82, 1.18, and 1.495. They are consistent with the $\frac{\alpha d}{2R^4}$ term known as the leading term in the interaction energy at R_e. Therefore, the charge-induced dipole interaction seems to be dominant at the equilibrium distance, R_e. Additionally, the equilibrium distance increases gradually from one complex to another as the RG's atomic number rises.

As can be noted from Table 3, for all Ba−RG complexes, the only available previous results for the anharmonic frequency

https://doi.org/10.1021/acsomega.3c08696
ACS Omega 2024, 9, 32407−32417

$\omega_e\chi_e$ and the rotational constant B_e for comparison are from the work of Buchachenko et al.[25] For all Ba−RG complexes, the TT values of B_e align well with the present CCSD(T) results, except in the case of Ba−He. Additionally, both present TT and CCSD(T) results show good agreement with the previous findings of Buchachenko et al..[25] For $\omega_e\chi_e$, TT values exhibit modest agreement with both the present CCSD(T) and the ECP/CBS/CCSD(T) results for Ba−Ar, Ba−Kr, and Ba−Xe. On the other hand, for the case of Ba−Xe, Abdessalem et al.[23] have reported values for $\omega_e\chi_e$ and B_e that reasonably match our findings.

For Ba−He, considerable variations emerge in different results. The differences in R_e, D_e, and ω_e obtained by the computational ab initio CCSD(T) and TT model potential are, respectively, 0.82 Å, 4.22 cm^{-1}, and 3.42 cm^{-1}. The ECP/CBS/CCSD(T) computations conducted by Buchachenko et al.[25] and the two pseudopotential studies, one by Czuchaj et al.[71] and the other by Brust and Greene,[72] produced well depths significantly smaller than those predicted by the current TT and CCSD(T) analyses. Conversely, our present findings align with the surface integral calculations of Kleinekathöfer.[70] The obtained TT ω_e aligns with the present CCSD(T) result, whereas it disagrees with the computational values reported by Buchachenko et al.[25]

In the case of Ba−Ne, concerning previous theoretical calculations, the TT values (R_e = 5.58 Å, D_e = 16 cm^{-1}, and ω_e = 7.99 cm^{-1}) exhibit good agreement with the ECP/CBS/CCSD(T) results (R_e = 5.815 Å, D_e = 12 cm^{-1}, and ω_e = 6.8 cm^{-1}) calculated by Buchachenko et al.[25] However, substantial differences were observed in comparison to the pseudopotential calculation of Czuchaj et al.,[21] where the pseudopotential values (D_e = 64 cm^{-1} and ω_e = 22 cm^{-1}) are four times and three times greater, respectively. Nevertheless, there is good agreement for the bond distance, with the present R_e = 5.58 Å closely matching the previous R_e = 5.34 Å, differing by only about 4%. Turning to the current CCSD(T) values (R_e = 5.61 Å, D_e = 39.07 cm^{-1}, and ω_e = 10.53 cm^{-1}), there is excellent agreement in R_e and ω_e, with differences of only 0.03 Å and 2.54 cm^{-1}, respectively. However, a modest agreement in D_e was noted, with a difference of 22.07 cm^{-1}.

Regarding Ba−Ar, the TT values of R_e = 5.61 Å and D_e = 60 cm^{-1} are in excellent agreement with the two previous ECP/CCSD(T) values (R_e = 5.62 Å and D_e = 54.2 cm^{-1}) by Davis and McCaffrey[5] and ECP/CBS/CCSD(T) values (R_e = 5.482 Å and D_e = 62.9 cm^{-1}) by Buchachenko et al.[25] General alignment is also observed with the theoretical results of Czuchaj et al.[21] and Issa et al.,[22] who used a similar theoretical approach involving CI/pseudopotential calculations to obtain R_e (Å)/D_e (cm^{-1}) values of 5.36/72.7 and 5.36/72.7, respectively. These two results are quite close to each other and are in agreement with the present study. The vibrational constant ω_e (13.75 cm^{-1}) is within reasonable consistency with the values of 16 cm^{-1} obtained by Czuchaj et al.,[21] 11.1 cm^{-1} obtained by Issa et al.,[22] and 11.3 cm^{-1} calculated by Buchachenko et al.[25] On the other hand, the ab initio CCSD(T) calculations have yielded the following results: a bond length of 5.75 Å, a bond energy of 47.03 cm^{-1}, and a harmonic frequency of 9.26 cm^{-1}. These values are in substantial agreement with the TT predicted values, with differences in R_e, D_e, and ω_e amounting to 0.14 Å, 13 cm^{-1}, and 4.49 cm^{-1}, respectively. Furthermore, a comparison with previous results reported in Table 3 reveals a strong alignment with the values presented in ref 5, where the difference in bond energy is only 7.17 cm^{-1}.

In the case of Ba−Kr, as illustrated in Table 3, the TT spectroscopic constants exhibit consistency with both the present ab initio CCSD(T) results and all previous theoretical calculations. Specifically, the TT values for R_e(Å)/D_e (cm^{-1}) of 5.63/87 are in good agreement with the values of 5.57/84, 5.72/80, and 5.387/101.4 obtained from the ECP/CCSD(T) investigation of Davis and McCaffrey,[5] the CI/pseudopotential calculation of Czuchaj et al.,[21] and the ECP/CBS/CCSD(T) results of Buchachenko et al.,[25] respectively. Regarding the present ab initio CCSD(T) calculations that resulted in R_e = 5.62 Å, D_e = 96.10 cm^{-1}, and ω_e = 9.87 cm^{-1}, an excellent agreement was noted with the ECP/CBS/CCSD(T) calculations of Buchachenko et al.,[25] particularly for D_e and ω_e, where the differences are 5.3 and 0.73 cm^{-1}, respectively. These results also align well with the values obtained from the TT model, with differences in R_e, D_e, and ω_e of only about 0.01 Å, 9 cm^{-1}, and 2.1 cm^{-1}, respectively. A general accordance can be observed with the two previous calculations in ref 5 and 21, where the difference in well depth is 12.1 cm^{-1}[73] and 16 cm^{-1}.[21]

For Ba−Xe, the current values of D_e = 123 cm^{-1} and R_e = 5.70 Å exhibit good agreement with the previous D_e (cm^{-1})/R_e (Å) results of 131.1/5.55 and 101/5.93, respectively, obtained by the calculations of Davis and McCaffrey[5] and Czuchaj et al.[21] A general agreement is also observed with the ECP/CBS/CCSD(T) values (R_e = 5.45 and D_e = 147.9 cm^{-1}) reported by Buchachenko et al.[25] However, the values of D_e = 427 cm^{-1} at R_e = 5.11 Å and ω_e = 17 cm^{-1} obtained from the pseudopotential calculation by Abdessalem et al.[23] differ significantly from our results and all previous theoretical findings. Turning to the present CCSD(T) calculations, the obtained values for R_e, D_e, and ω_e are 5.69 Å, 113.88 cm^{-1}, and 9.40 cm^{-1}, respectively. These results exhibit significant agreement with those derived from the TT model potential. Remarkably, the variance in R_e is only 0.01 Å, while differences of 10 and 2.77 cm^{-1} are observed for D_e and ω_e, respectively. An agreement in D_e is also evident when compared to the earlier results presented in ref 5 and 21, where the differences are approximately 12 and 18 cm^{-1}, respectively.

The results obtained from the TT model potential in conjunction with the combining rules demonstrate a good agreement with both the current CCSD(T) calculations and previous theoretical findings from various ab initio methods.

3.2. Trends in the κ Parameter for AE−RG and AE^+−RG.

To analyze and comprehend the distinctions in interactions, we employ the κ[74] parameter (also known as the Sutherland parameter), originally introduced in 1938[75] and symbolized as Δ in the work published by Xie and Hsu.[76] This parameter signifies the potential reduced curvature at the equilibrium distance R_e and is mathematically expressed as follows

$$\kappa = \frac{R_e^2}{D_e}\left(\frac{d^2V(R)}{dR^2}\right)_{R_e} = \frac{R_e^2}{D_e}k_e \tag{43}$$

In terms of spectroscopic constants ω_e, B_e, and D_e, this equation can be further represented as

$$\kappa = \frac{\omega_e^2}{2B_eD_e} \tag{44}$$

Before we delve into the results, it is worth noting that in ref 74, Winn determined the values of κ for various types of molecular systems. Winn's findings revealed that the κ parameter consistently maintains a relatively low value for

https://doi.org/10.1021/acsomega.3c08696
ACS Omega 2024, 9, 32407−32417

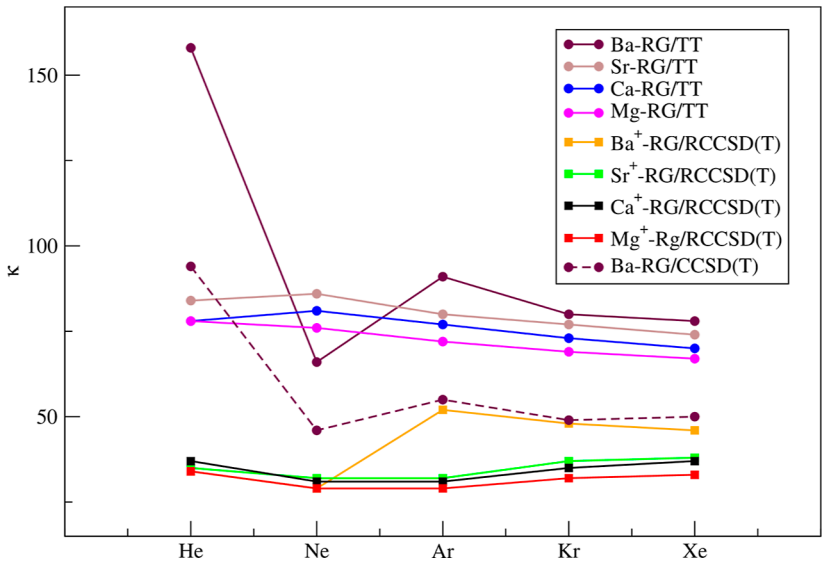

Figure 2. Plot of the κ parameter for AE/AE$^+$−RG (AE = Ba, Sr, Ca, and Mg and RG = He, Ne, Ar, Kr, and Xe).

strongly bound chemical systems. In contrast, for weakly bound molecular systems, this parameter is found to be large, even huge, compared to the previous case.

Figure 2 reports the κ parameter for Ba−RG, computed using spectroscopic values derived from both ab initio CCSD(T) and TT potential, and for analogous AE−RG systems (AE = Sr, Ca, Mg), computed using spectroscopic values derived from the TT model potential.[30,34,35] These molecular systems all share the common characteristic of being isoelectronic with closed electron shells. Additionally, the same figure showcases κ values for one-electron AE$^+$−RG (AE = Ba, Sr, Ca, and Mg) systems. To determine κ for these ionic systems, we utilized the previous spectroscopic constants derived from the RCCSD(T) potentials.[77−79] In cases where the rotational constant B_e was not available for Sr−RG and Ca−RG, we derived it by employing data from refs 30 and 31 along with the following formula

$$B_e = \frac{1}{2\mu R_e^2} \tag{45}$$

As illustrated in Figure 2, it is evident that κ is not a constant parameter. Nonetheless, κ values within the same AE−RG and AE$^+$−RG series are remarkably close to each other, displaying consistent trends, with the exception of AE/AE$^+$ = Ba/Ba$^+$. Within the AE−RG complexes, there is a pronounced similarity in trends, showing a decreasing κ value with an increase in the atomic number of RG, except for the minor increase from AE−He to AE−Ne. For Ba−RG, although the shift of the κ values derived from ab initio CCSD(T) to lower values is notable, they exhibit similar trends to those obtained from the TT model. In both cases, while the κ values for Ba−Ar, Ba−Kr, and Ba−Xe complexes seem to align well with the expected range, Ba−He exhibits a significantly higher value and Ba−Ne shows a notably lower κ value compared to those of the other complexes.

Turning our attention to ionic systems involving AE$^+$ and RG, we consistently observe a trend in the κ parameter. In most cases, except for Ba$^+$−RG, this parameter increases with the atomic number of the RG atom, with the only exception being a minor decrease from AE$^+$−He to AE$^+$−Ne. The rise in the κ value as the atomic number of the RG atom increases can be attributed to the potential becoming "harder". For Ba$^+$−RG, the κ parameter behavior generally aligns with that of Ba−RG molecular complexes, despite the fact that Ba$^+$−He and Ba$^+$−Ne exhibit values well within the expected range for AE$^+$−RG interactions. Notably, there is a significant increase in the levels between Ba$^+$−Ne and Ba$^+$−Ar.

The variance in the observed behavior of the κ parameter can be attributed to the disparate charge distribution of atoms, as elucidated by Gardner et al.[79]

4. CONCLUSIONS

The PECs and the spectroscopic constants of the Ba−RG (RG = He−Xe) complexes have been calculated by the analytical model of Tang and Toennies and a set of combining rules. For the short-range Born−Mayer repulsive coefficients A and b, we used the combining rules proposed by Böhm−Ahlrichs, while for long-range dispersion coefficients C_6, C_8, and C_{10}, we used combining rules based on the Casimir−Polder theory.

To check the validity of the used model, in addition to the comparison with the previously available experimental and theoretical studies, we have carried out an ab initio calculation at the CCSD(T) level of theory and large basis sets. In general, our calculations are within the range of both the present ab initio CCSD(T) and previous published calculations. Considering the simplicity of the TT model potential, there is a remarkably good performance of the use of the combining rules approach. Consequently, the present method should be used largely, at least as a starting point for the interplay between theory and experiment. Mathematically, the present potential is an entire function in which derivatives exist everywhere and to all orders. It can be easily used in theories requiring an analytic extension into the complex plane such as theories of predissociation of van der Waals complexes.

To understand the differences in interactions between different kinds of bonds, we calculated and plotted the curvatives of the constant κ known as the Sutherland parameter. This study is realized for AE−RG (AE = Mg, Sr, Ca, Ba and RG = He−Xe) and their corresponding monocation systems AE$^+$−RG. Except for the cases of Ba$^+$−RG and Ba−RG complexes, we observed that the two types of neutral and ionic complexes have opposite tendencies. Going from He to Xe, the curves of constant κ for the neutral AE−RG complexes are decreasing, whereas those of the AE$^+$−RG complexes are increasing.

https://doi.org/10.1021/acsomega.3c08696
ACS Omega 2024, 9, 32407−32417

■ ASSOCIATED CONTENT

Supporting Information

The Supporting Information is available free of charge at https://pubs.acs.org/doi/10.1021/acsomega.3c08696.

PEC data for barium (Ba) interacting with various noble gas atoms (He, Ne, Ar, Kr, and Xe) computed at the CCSD(T) level of theory (PDF)

■ AUTHOR INFORMATION

Corresponding Authors

Samah Saidi − *Department of Physics, College of Science and Humanities in Al-Kharj, Prince Sattam bin Abdulaziz University, Al-Kharj 11942, Saudi Arabi; Laboratory of Interfaces and Advanced Materials Physics Department Faculty of Science, University of Monastir, Monastir 5019, Tunisia*; Email: s.saidi@psau.edu.sa

Mohamed Bejaoui − *Laboratory of Interfaces and Advanced Materials Physics Department Faculty of Science, University of Monastir, Monastir 5019, Tunisia*; orcid.org/0009-0002-7446-2999; Email: Mohamed.Bejaoui@ipeim.rnu.tn

Hamid Berriche − *Department of Mathematics and Physics School of Arts and Science, American University of Ras Al Khaimah, Ras Al Khaimah 10021, UAE; Laboratory of Interfaces and Advanced Materials Physics Department Faculty of Science, University of Monastir, Monastir 5019, Tunisia*; orcid.org/0000-0002-1442-669X; Email: hamid.berriche@aurak.ac.ae

Complete contact information is available at: https://pubs.acs.org/10.1021/acsomega.3c08696

Notes

The authors declare no competing financial interest.

■ ACKNOWLEDGMENTS

The authors extend their appreciation to Prince Sattam bin Abdulaziz University for funding this research work through the project number PSAU/2023/01/25573.

■ REFERENCES

(1) Mong, B.; Cook, S.; Walton, T.; Chambers, C.; Craycraft, A.; Benitez-Medina, C.; Hall, K.; Fairbank, W.; Albert, J. B.; Auty, D. J.; et al. Spectroscopy of Ba and Ba^+ deposits in solid xenon for barium tagging in nEXO. *Phys. Rev. A* **2015**, *91*, 022505.

(2) Auger, M. Search for Neutrinoless Double-Beta Decay in ^{136}Xe with EXO-200. *Phys. Rev. Lett.* **2012**, *109*, 032505.

(3) Davis, B. M.; Gervais, B.; McCaffrey, J. G. An investigation of the sites occupied by atomic barium in solid xenon—A 2D-EE luminescence spectroscopy and molecular dynamics study. *J. Chem. Phys.* **2018**, *148*, 124308.

(4) Davis, B.; McCaffrey, J. G. Luminescence of Atomic Barium in Rare Gas Matrices: A Two-Dimensional Excitation/Emission Spectroscopy Study. *J. Phys. Chem. A* **2018**, *122*, 7339−7350.

(5) Davis, B. M.; McCaffrey, J. G. Absorption spectroscopy of heavy alkaline earth metals Ba and Sr in rare gas matrices—CCSD(T) calculations and atomic site occupancies. *J. Chem. Phys.* **2016**, *144*, 044308.

(6) Loginov, E.; Drabbels, M. Spectroscopy and dynamics of barium-doped helium nanodroplets. *J. Chem. Phys.* **2012**, *136*, 154302.

(7) Zhang, X.; Drabbels, M. Communication: Barium ions and helium nanodroplets: Solvation and desolvation. *J. Chem. Phys.* **2012**, *137*, 051102.

(8) Lebedev, V.; Moroshkin, P.; Weis, A. Spectroscopy of barium atoms in liquid and solid helium matrices. *Phys. Rev. A* **2011**, *84*, 022502.

(9) Masson, A.; Poisson, L.; Gaveau, M.-A.; Soep, B.; Mestdagh, J.-M.; Mazet, V.; Spiegelman, F. Dynamics of highly excited barium atoms deposited on large argon clusters. I. General trends. *J. Chem. Phys.* **2010**, *133*, 054307.

(10) Briant, M.; Gaveau, M.-A.; Mestdagh, J.-M. Observation of a barium xenon exciplex within a large argon cluster. *J. Chem. Phys.* **2010**, *133*, 034306.

(11) Kielkopf, J. The interaction of excited states of barium with xenon atoms determined by spectral-line contour measurements. *J. Phys. B: At. Mol. Phys.* **1978**, *11*, 25−36.

(12) Harima, H.; Tachibana, K.; Urano, Y. Empirical interatomic potentials for Ba-rare-gas systems deduced from an absorption measurement. *J. Phys. B: At. Mol. Phys.* **1982**, *15*, 3679−3693.

(13) Ehrlacher, E.; Huennekens, J. Noble-gas broadening rates for the $6s^2\,^1S_0 \rightarrow 6s6p\ ^{1,3}P_1$ resonance and intercombination lines of barium. *Phys. Rev. A* **1993**, *47*, 3097−3104.

(14) Breckenridge, W. H.; Merrow, C. N. Exclusive production of Ba(6s6p3P2) in the collisional deactivation of Ba(6s6p1P1) by the rare gases. *J. Chem. Phys.* **1988**, *88*, 2329−2333.

(15) Visticot, J. P.; Berlande, J.; Cuvellier, J.; Mestdagh, J. M.; Meynadier, P.; de Pujo, P.; Sublemontier, O.; Bell, A. J.; Frey, J. G. Energy dependence of the inelastic process Ba(6s6p1P1)+Ar,He → Ba(6s6p3P1,2)+Ar,He. *J. Chem. Phys.* **1990**, *93*, 5354−5355.

(16) Ehrlacher, E.; Huennekens, J. Excitation transfer among, and quenching of, the barium 6s5d ^3D_J metastable levels due to collisions with argon, nitrogen, and barium perturbers. *Phys. Rev. A* **1994**, *50*, 4786−4793.

(17) Vadla, C.; Niemax, K.; Horvatic, V.; Beuc, R. Population and deactivation of lowest lying barium levels by collisions with He, Ar, Xe and Ba ground state atoms. *Z. Phys. D: At., Mol. Clusters* **1995**, *34*, 171−184.

(18) Brust, J.; Gallagher, A. C. Excitation transfer in barium by collisions with noble gases. *Phys. Rev. A* **1995**, *52*, 2120−2131.

(19) Namiotka, R. K.; Ehrlacher, E.; Sagle, J.; Brewer, M.; Namiotka, D. J.; Hickman, A. P.; Streater, A. D.; Huennekens, J. Diffusion of barium atoms in the 6s5d^3D_J metastable levels and the $6s^2\,^1S_0$ ground state through noble-gas perturbers. *Phys. Rev. A* **1996**, *54*, 449−461.

(20) Smedley, J. E.; Coulter, S. K.; Felton, E. J.; Zomlefer, K. S. Collisional Deactivation of Ba 5d7p 3D1 by Noble Gases. *J. Phys. Chem. A* **2008**, *112*, 9526−9530.

(21) Czuchaj, E.; Rebentrost, F.; Stoll, H. e. a.; Preuss, H. Calculation of ground- and excited-state potential energy curves for barium-rare gas complexes in a pseudopotential approach. *Theor. Chem. Acc.* **1998**, *100*, 117−123.

(22) Issa, K.; Dardouri, R.; Oujia, B. Theoretical Study of the BaAr Molecule and Its Ion Ba+Ar: Potential Energy Curves and Spectroscopic Constants. *Surf. Interfaces Mater.* **2013**, *1*, 15−22.

(23) Abdessalem, K.; Mejrissi, L.; Issaoui, N.; Oujia, B.; Gadéa, F. X. One and Two-Electron Investigation of Electronic Structure for Ba+Xe and BaXe van der Waals Molecules in a Pseudopotential Approach. *J. Phys. Chem. A* **2013**, *117*, 8925−8938.

(24) Abdessalem, K.; Mejrissi, L.; Habli, H.; Issaoui, N.; Ghalla, H.; Oujia, B. Spectroscopic and electric dipole properties of the Van der Waals interaction between barium and krypton atoms. *Mol. Phys.* **2019**, *117*, 143−157.

(25) Buchachenko, A. A.; Viehland, L. A. Interaction potentials and transport properties of Ba, Ba+, and Ba2+ in rare gases from He to Xe. *J. Chem. Phys.* **2018**, *148*, 154304.

(26) Xian, W.-Q.; Zhang, Z.-P.; Tu, Z.-Y.; Zhou, H.; Li, L.-B.; Chen, A.-M. Theoretical study of the spectroscopic constants of the ground state of the diatomic Ba-RG (RG = Kr, Xe, Rn) based on the coupled cluster theory with spin−orbit coupling. *J. Phys. B: At., Mol. Opt. Phys.* **2023**, *56*, 115102.

(27) Tang, K. T.; Toennies, J. P. An improved simple model for the van der Waals potential based on universal damping functions for the dispersion coefficients. *J. Chem. Phys.* **1984**, *80*, 3726−3741.

(28) Tang, K. T.; Toennies, J. P. The van der Waals potentials between all the rare gas atoms from He to Rn. *J. Chem. Phys.* **2003**, *118*, 4976−4983.

(29) Li, P.; Xie, W.; Tang, K. T. The van der Waals potential of the magnesium dimer. *J. Chem. Phys.* **2010**, *133*, 084308.
(30) Yang, D. D.; Li, P.; Tang, K. T. The ground state van der Waals potentials of the calcium dimer and calcium rare-gas complexes. *J. Chem. Phys.* **2009**, *131*, 154301.
(31) Yin, G. P.; Li, P.; Tang, K. T. The ground state van der Waals potentials of the strontium dimer and strontium rare-gas complexes. *J. Chem. Phys.* **2010**, *132*, 074303.
(32) Li, P.; Ren, J.; Niu, N.; Tang, K. T. Corresponding States Principle for the Alkaline Earth Dimers and the van der Waals Potential of Ba2. *J. Phys. Chem. A* **2011**, *115*, 6927−6935.
(33) Wei, L. M.; Li, P.; Duan, W.; Yang, H.; Wen, Y.; Jin, F. The ground state van der Waals potentials of Zn-RG complexes (RG = He, Ne, Ar, Kr, Xe). *Chem. Phys. Lett.* **2020**, *741*, 137099.
(34) Saidi, S.; Alharzali, N.; Berriche, H. A combining rule calculation of the ground-state van der Waals potentials of the magnesium rare-gas complexes. *Mol. Phys.* **2017**, *115*, 931−941.
(35) Sheng, X. W.; Li, P.; Tang, K. T. A combining rule calculation of the ground state van der Waals potentials of the mercury rare-gas complexes. *J. Chem. Phys.* **2009**, *130*, 174310.
(36) Tang, K. T.; Norbeck, J. M.; Certain, P. R. Upper and lower bounds of two- and three-body dipole, quadrupole, and octupole van der Waals coefficients for hydrogen, noble gas, and alkali atom interactions. *J. Chem. Phys.* **1976**, *64*, 3063−3074.
(37) Kumar, A.; Meath, W. J. Integrated dipole oscillator strengths and dipole properties for Ne, Ar, Kr, Xe, HF, HCl, and HBr. *Canad. J. Chemistry* **1985**, *63*, 1616−1630.
(38) Thakkar, A. J.; Hettema, H.; Wormer, P. E. S. Ab initio dispersion coefficients for interactions involving rare-gas atoms. *J. Chem. Phys.* **1992**, *97*, 3252−3257.
(39) Aziz, R. A. *Inert Gases: Potentials, Dynamics, and Energy Transfer in Doped Crystals*; Klein, M. L., Ed.; *Springer Series in Chemical Physics*; Springer, 1984; pp 5−86.
(40) Toennies, J. P. On the validity of a modified Buckingham potential for the rare gas dimers at intermediate distances. *Chem. Phys. Lett.* **1973**, *20*, 238−241.
(41) Born, M.; Mayer, J. Zur Gittertheorie der Ionenkristalle. *Z. Phys.* **1932**, *75*, 1−18.
(42) Gilbert, T. L. Soft-Sphere Model for Closed-Shell Atoms and Ions. *J. Chem. Phys.* **1968**, *49*, 2640−2642.
(43) Gilbert, T. L.; Simpson, O. C.; Williamson, M. A. Relation between charge and force parameters of closed-shell atoms and ions. *J. Chem. Phys.* **1975**, *63*, 4061−4071.
(44) Smith, F. T. Atomic Distortion and the Combining Rule for Repulsive Potentials. *Phys. Rev. A* **1972**, *5*, 1708−1713.
(45) Böhm, H.-J.; Ahlrichs, R. A study of short-range repulsions. *J. Chem. Phys.* **1982**, *77*, 2028−2034.
(46) Mavroyannis, C.; Stephen, M. Dispersion forces. *Mol. Phys.* **1962**, *5*, 629−638.
(47) McLachlan, A. D. Retarded dispersion forces between molecules. *Proc. R. Soc. London, Ser. A* **1963**, *271*, 387−401.
(48) Dalgarno, A. New methods for calculating long-range intermolecular forces. *Adv. Chem. Phys.* **1967**, *12*, 143−166.
(49) Tang, K. T. Dynamic Polarizabilities and van der Waals Coefficients. *Phys. Rev.* **1969**, *177*, 108−114.
(50) *Mathematical Methods for Engineers and Scientists 3: Fourier Analysis, Partial Differential Equations and Variational Methods*; Tang, K.-T., Ed.; Springer, 2007; pp 111−162.
(51) Tang, K. T.; Toennies, J. P. New combining rules for well parameters and shapes of the van der Waals potential of mixed rare gas systems. *Z. Phys. D: At., Mol. Clusters* **1986**, *1*, 91−101.
(52) Porsev, S. G.; Derevianko, A. High-accuracy calculations of dipole, quadrupole, and octupole electric dynamic polarizabilities and van der Waals coefficients C6, C8, and C10 for alkaline-earth dimers. *J. Exp. Theor. Phys.* **2006**, *102*, 195−205.
(53) Kaur, S.; Mahajan, C. G. *Pramana − Journal of Physics | Indian Academy of Sciences*, 2002. https://www.ias.ac.in/describe/article/pram/059/03/0479-048web6.
(54) Dunham, J. L. The Energy Levels of a Rotating Vibrator. *Phys. Rev.* **1932**, *41*, 721−731.
(55) Herschbach, D. R.; Laurie, V. W. Anharmonic Potential Constants and Their Dependence upon Bond Length. *J. Chem. Phys.* **1961**, *35*, 458−464.
(56) Pritchard, B. P.; Altarawy, D.; Didier, B.; Gibson, T. D.; Windus, T. L. New Basis Set Exchange: An Open, Up-to-Date Resource for the Molecular Sciences Community. *J. Chem. Inf. Model.* **2019**, *59*, 4814−4820.
(57) Feller, D. The role of databases in support of computational chemistry calculations. *J. Comput. Chem.* **1996**, *17*, 1571−1586.
(58) Schuchardt, K. L.; Didier, B. T.; Elsethagen, T.; Sun, L.; Gurumoorthi, V.; Chase, J.; Li, J.; Windus, T. L. Basis Set Exchange: A Community Database for Computational Sciences. *J. Chem. Inf. Model.* **2007**, *47*, 1045−1052.
(59) Dunning, T. H. Gaussian basis sets for use in correlated molecular calculations. I. The atoms boron through neon and hydrogen. *J. Chem. Phys.* **1989**, *90*, 1007−1023.
(60) Kendall, R. A.; Dunning, T. H.; Harrison, R. J. Electron affinities of the first-row atoms revisited. Systematic basis sets and wave functions. *J. Chem. Phys.* **1992**, *96*, 6796−6806.
(61) van Mourik, T.; Wilson, A. K.; Dunning, T. H. Benchmark calculations with correlated molecular wavefunctions. XIII. Potential energy curves for He2, Ne2 and Ar2 using correlation consistent basis sets through augmented sextuple zeta. *Mol. Phys.* **1999**, *96*, 529−547.
(62) Woon, D. E.; Dunning, T. H., Jr. unpublished. As referenced in 'van Mourik et al. Mol. Phys. 1999, 96, 529−547.
(63) *Energy-consistent Pseudopotentials of the Stuttgart/Cologne Group*. 2014. https://www.tc.uni-koeln.de/PP/clickpse.en.htmwebl.
(64) Peterson, K. A.; Figgen, D.; Goll, E.; Stoll, H.; Dolg, M. Systematically convergent basis sets with relativistic pseudopotentials. II. Small-core pseudopotentials and correlation consistent basis sets for the post-d group 16−18 elements. *J. Chem. Phys.* **2003**, *119*, 11113−11123.
(65) Weigend, F.; Baldes, A. Segmented contracted basis sets for one- and two-component Dirac−Fock effective core potentials. *J. Chem. Phys.* **2010**, *133*, 174102.
(66) Peterson, K. A.; Figgen, D.; Dolg, M.; Stoll, H. Energy-consistent relativistic pseudopotentials and correlation consistent basis sets for the 4d elements Y−Pd. *J. Chem. Phys.* **2007**, *126*, 124101.
(67) Lim, I. S.; Schwerdtfeger, P.; Metz, B.; Stoll, H. All-electron and relativistic pseudopotential studies for the group 1 element polarizabilities from K to element 119. *J. Chem. Phys.* **2005**, *122*, 104103.
(68) Lim, I. S.; Stoll, H.; Schwerdtfeger, P. Relativistic small-core energy-consistent pseudopotentials for the alkaline-earth elements from Ca to Ra. *J. Chem. Phys.* **2006**, *124*, 034107.
(69) Werner, H.-J.; Knowles, P. J.; Knizia, G.; Manby, F. R.; Schütz, M. Molpro: a general-purpose quantum chemistry program package. *Wiley Interdiscip. Rev.: Comput. Mol. Sci.* **2012**, *2*, 242−253.
(70) Kleinekathöfer, U. Ground state potentials for alkaline-earth−helium diatoms calculated by the surface integral method. *Chem. Phys. Lett.* **2000**, *324*, 403−410.
(71) Czuchaj, E.; Rebentrost, F.; Stoll, H.; Preuss, H. Pseudopotential calculations for the potential energies of LiHe and BaHe. *Chem. Phys.* **1995**, *196*, 37−46.
(72) Brust, J.; Greene, C. H. Theoretical investigation of barium-helium collisions. I. The adiabatic potential curves. *Phys. Rev. A* **1997**, *56*, 2005−2012.
(73) Breckenridge, W.; Jouvet, C.; Soep, B. Metal-atom/rare-gas van der Waals complexes. *Adv. Met. Semicond. Clusters* **1996**, *3*, 1−83.
(74) Winn, J. S. A systematic look at weakly bound diatomics. *Acc. Chem. Res.* **1981**, *14*, 341−348.
(75) Sutherland, G. B. The relation between the force constant, the inter-nuclear distance, and the dissociation energy of a diatomic linkage. *Proc. Indian Natl. Sci. Acad., Part A* **1938**, *8*, 341−344.
(76) Xie, R.-H.; Hsu, P. S. Universal Reduced Potential Function for Diatomic Systems. *Phys. Rev. Lett.* **2006**, *96*, 243201.
(77) McGuirk, M. F.; Viehland, L. A.; Lee, E. P. F.; Breckenridge, W. H.; Withers, C. D.; Gardner, A. M.; Plowright, R. J.; Wright, T. G.

https://doi.org/10.1021/acsomega.3c08696
ACS Omega 2024, 9, 32407−32417

Theoretical study of Ban+−RG (RG = raregas) complexes and transport of Ban+ through RG (n = 1,2;RG = He−Rn). *J. Chem. Phys.* **2009**, *130*, 194305.
(78) Gardner, A. M.; Withers, C. D.; Wright, T. G.; Kaplan, K. I.; Chapman, C. Y. N.; Viehland, L. A.; Lee, E. P. F.; Breckenridge, W. H. Theoretical study of the bonding in Mn+-RG complexes and the transport of Mn+ through rare gas (M = Ca, Sr, and Ra; n = 1 and 2; and RG = He−Rn). *J. Chem. Phys.* **2010**, *132*, 054302.
(79) Gardner, A. M.; Withers, C. D.; Graneek, J. B.; Wright, T. G.; Viehland, L. A.; Breckenridge, W. H. Theoretical Study of M+RG and M2+RG Complexes and Transport of M+ through RG (M = Be and Mg, RG = HeRn). *J. Phys. Chem. A* **2010**, *114*, 7631−7641.

https://doi.org/10.1021/acsomega.3c08696
ACS Omega 2024, 9, 32407−32417